Structural Complexities in the Active Layers of Organic Electronics

Stephanie S. Lee and Yueh-Lin Loo

Department of Chemical Engineering, Princeton University, Princeton, New Jersey 08544; email: lloo@princeton.edu

Annu. Rev. Chem. Biomol. Eng. 2010. 1:59–78

First published online as a Review in Advance on January 4, 2010

The *Annual Review of Chemical and Biomolecular Engineering* is online at chembioeng.annualreviews.org

This article's doi:
10.1146/annurev-chembioeng-073009-100851

1947-5438/10/0715-0059$20.00

Key Words

organic thin film transistors, organic photovoltaics, organic light-emitting diodes, morphology and structure, processing-structure-function relationships

Abstract

The field of organic electronics has progressed rapidly in recent years. However, understanding the direct structure-function relationships between the morphology in electrically active layers and the performance of devices composed of these materials has proven difficult. The morphology of active layers in organic electronics is inherently complex, with heterogeneities existing across multiple length scales, from subnanometer to micron and millimeter range. A major challenge still facing the organic electronics community is understanding how the morphology across all of the length scales in active layers collectively determines the device performance of organic electronics. In this review we highlight experiments that have contributed to the elucidation of structure-function relationships in organic electronics and also point to areas in which knowledge of such relationships is still lacking. Such knowledge will lead to the ability to select active materials on the basis of their inherent properties for the fabrication of devices with prespecified characteristics.

INTRODUCTION

The use of organic semiconducting small molecules and polymers as the active layers in electronic devices has garnered much attention over the past few decades. Not only can these materials potentially lead to inexpensive, large-area electronic devices with flexible form factors, such as display panels (1–3), radio frequency identification (RFID) tags (4, 5), and biological sensors (6, 7), but they may also be incorporated into cost-effective devices for harvesting sunlight to help meet the world's growing energy needs (8, 9). Organic and polymer semiconductors differ from their inorganic counterparts in their synthetic versatility; organics can be chemically functionalized and derivatized via straightforward chemical routes to impart tunability to their physical, mechanical, optical, and electronic properties (10, 11). Furthermore, organic semiconductors can be deposited easily onto rigid substrates or mechanically flexible plastics (12, 13) at near-ambient conditions using a variety of conventional processing methods, such as spin coating, thermal evaporation, and those conducive to roll-to-roll processing, such as inkjet printing, screen printing, and gravure printing (14–16). These qualities, which are unique to organics, promise the realization of ubiquitous, low-cost electronic devices for everyday use and will usher in the so-called "electronics anywhere" (17) era. It is this excitement that has driven tremendous progress in the field.

Intensive research efforts in the organic electronics community have focused on improving the device performance of organic thin film transistors (OTFTs), bulk-heterojunction organic photovoltaics (OPVs), and organic light-emitting diodes (OLEDs). The mobilities of OTFTs now rival those of amorphous silicon devices (18). The efficiencies of OPVs are closer to reaching the 10% that is needed for commercialization (8, 16, 19, 20), with tandem solar cells recently achieving efficiencies as high as 6.5% (9). OLEDs are currently being mass produced, with luminance levels in some cases far exceeding the minimum 100 cd m^{-2} required for many commercial devices (3).

However, improvements in device characteristics have thus far chiefly been arrived at through an Edisonian, trial-and-error approach (21, 22). Although it is commonly accepted that the details of the morphology in the active layers of devices can influence device performance and general guidelines describing how processing conditions can influence the structure of active layers exist, we still lack a fundamental understanding of detailed processing-structure-function relationships that will allow the prediction of device properties a priori. A major challenge in obtaining such knowledge lies in the inherent structural complexities of organic semiconductor thin films. These active layers are composed of one organic semiconductor in the case of most OTFTs, and a blend of two or more constituents in OPVs and OLEDs. During film formation, via either thermal evaporation or solution deposition, thermodynamic driving forces induce crystallization of organic and polymer semiconductors as well as phase separation of chemically dissimilar species. Kinetic limitations that arise from solvent evaporation and high thermal deposition flux, however, can trap the active layers in states far from equilibrium, leading to much more morphological complexity.

The structural heterogeneities in the active layers within organic electronic devices exist at multiple length scales, as visualized in **Figure 1**. At the molecular level, small molecules or polymer chains must orient to crystallize; misalignment or the presence of vacancies can cause defects. At the nanometer to micron length scale, crystalline regions bordered by grain boundaries can vary in size and orientation. At the largest length scale, which can span tens of nanometers to hundreds of microns, two organic semiconductors can demix to form chemically distinct regions. The structural heterogeneities at each of these length scales can critically impact the electronic processes within the active layers during device operation. Much research has therefore focused on visualizing and quantifying the structural complexities in organic semiconductor thin films. Currently, most characterization tools used to study the active layers of organic electronics probe structure only at a single length scale. To understand fully the structure-function relationships

between the morphology in the active layers and the device performance of organic electronics, however, it is necessary to examine the hierarchical structuring of organic semiconductor thin films that traverses all these length scales. In doing so, we will be able to determine how the morphologies at each length scale combine to determine overall device performance.

In this review, we highlight research in the field of organic electronics with particular focus on the elucidation of structure-function relationships at the individual length scales shown in **Figure 1**. In doing so, we survey cutting-edge techniques that are being developed specifically for the study of organic semiconductor thin films. Looking forward, studies that probe across multiple length scales will greatly enhance our knowledge of how morphology in the active layers of organic electronics impacts device performance. Ultimately, the ability to probe charge transport directly within active layers during device operation while simultaneously collecting morphological information will allow for direct and unambiguous correlation between structure and function in the active layers of organic electronics. Such know-how should generate guidelines and design rules for the synthesis of new materials and the development of processes to control the structuring of active layers, which should ultimately result in the realization of devices with prespecified characteristics.

MOLECULAR ORDERING

Given the extensive conjugation and thus rigidity of organic semiconducting small molecules and polymers, these materials often have a strong driving force to crystallize in the solid state. The extent and quality of crystallization, however, depend strongly on the processing conditions used to deposit these materials. For instance, when organic semiconductors and polymers are deposited from solution, rapid solvent evaporation can severely limit molecular motion, effectively vitrifying the molecules in kinetically-trapped states that contain extensive disorder. At one extreme is triethylsilylethynyl anthradithiophene (TES ADT), a small-molecule organic semiconductor that deposits as a completely amorphous film when spin coated from toluene despite its strong tendency to crystallize under other film-forming circumstances (23–25).

In this section we demonstrate the importance of molecular ordering in the active layers of organic electronics. We also highlight challenges still facing the organic electronics community in probing the structure of organic semiconductor thin films at this length scale.

Impact of Molecular Ordering on Device Mobility

In organic semiconductor thin films, charge carriers are transported through π-orbital overlap of conjugated small molecules or polymer chains. Alignment of the organic semiconductor over significant distances in the active layers, or crystallization, is thus crucial, for this process maximizes π-orbital overlap, allowing efficient charge transfer from molecule to molecule or chain to chain. Conversely, defects within organic semiconductor crystals, such as misalignment of molecules, vacancies, and dislocations, can disrupt the π-orbital overlap network, increasing the barrier to intermolecular charge transport.

It is generally accepted that increased crystallinity in the active layers of organic electronics improves charge transport, thereby enhancing device mobility (23, 26–38). For example, exposure of amorphous TES ADT films to dichloroethane vapor imparts molecular motion to the molecules; TES ADT is then able to crystallize (23). This change in morphology in the active layers brings about an enhancement in device mobility: The mobility of OTFTs containing amorphous TES ADT in their active layers is 0.002 $cm^2\ V^{-1}\ s^{-1}$ compared with 0.1 $cm^2\ V^{-1}\ s^{-1}$ for similar devices in which TES ADT is crystallized via solvent vapor annealing (23). Thermal annealing

of organic semiconductor thin films can also impart molecular motion to organic semiconductor small molecules or polymer chains, which allows molecular rearrangement in the active layers (32, 33). In the case of pentacene OTFTs, thermal annealing of the active layers can improve device mobility from 0.19 $cm^2\ V^{-1}\ s^{-1}$ to 0.49 $cm^2\ V^{-1}\ s^{-1}$ by enhancing the degree of ordering of the molecules (32).

Inducing preferential orientation in substrates prior to organic semiconductor deposition has also been reported to improve molecular ordering in the channels of OTFTs, thereby enhancing device mobilities. In these examples, the substrates are prealigned via photoalignment, a process in which the polymer substrate is aligned with linearly polarized UV light (30). Mechanical rubbing, a process inspired by analogous techniques used to align liquid crystals in the display industry, can also facilitate alignment of substrates (28, 38–40). Similar to the epitaxial growth of inorganics, the organic semiconductor that is deposited on these prealigned substrates adopts a preferential orientation owing to the underlying anisotropy. For example, mechanically rubbing the self-assembled monolayer (SAM) that is preadsorbed on the substrate surface can direct molecular ordering in subsequently deposited pentacene molecules (38). OTFTs composed of pentacene thin films deposited on rubbed SAMs rather than unrubbed SAMs display a device mobility that is 15 times higher, suggesting the strong influence of molecular ordering of the organic semiconductor on charge transport through the active layers of OTFTs.

However, there are counterexamples that show that increased molecular ordering in the active layers can be detrimental to the device performance of organic electronics. It is generally accepted, for example, that increased crystallinity in the active layers of OLED devices can cause a decrease in luminance (41). In OLEDs, electrons and holes are injected into the active layers, which are often composed of a blend of two organic semiconductors, from the respective electrodes. Depending on the energy levels of the organic semiconductors, transport of electrons and holes through the active layers can occur in one or both of the phases (42). Charge carriers then must recombine at the interface between the phase-separated domains to emit light. Although crystallization of either or both phases can improve charge transport by increasing π-orbital overlap, crystallization often induces large-scale phase separation between the two components of the active layers. This phenomenon effectively decreases the interfacial area between the two polymers, thereby reducing the quantity of charge carrier recombination events that result in light generation.

In an effort to examine this phenomenon in more detail, studies of adsorbed layers composed of a blend of 1,4-bis(benzothiazole-vinyl) benzene (BT) and 2,2′,2″-(1,3,5-phenylene)tris-[1-phenyl-1H-benzimidazole] (TPBI) were carried out on highly oriented pyrolytic graphite (41). The adlayers were imaged with subnanometer resolution by scanning tunneling microscopy (STM) before and after thermal annealing (**Figures 2*a*** and ***b***, respectively). Focusing on the crystalline regions in the STM images of **Figure 2*b*** reveals that thermal annealing increases molecular ordering in the BT phase (labeled I), whereas the surrounding TPBI-rich phase remains amorphous (labeled II). Corresponding photoemission experiments on similarly prepared adlayers reveal a decrease in photoluminescence intensity for thermally annealed adlayers compared with unannealed adlayers.

In this case, thermal annealing, which induces the crystallization of BT, necessarily increases the extent of phase separation between BT and TPBI. Although charge transport is improved within individual crystals of BT, this process effectively decreases the amount of BT/TPBI interface at which charges can recombine to emit light. This example illustrates how crystallization of one species can influence phase separation within active layers and vice versa—a clear indication of the structural complexities in such systems. It also demonstrates the importance of elucidating the hierarchical structural development over multiple length scales to obtain a complete picture of the causal relationships between morphology and device characteristics.

Challenges in Imaging Organic Electronic Active Layers at the Molecular Level

STM imaging of BT/TPBI adlayers provides important insights on how morphology at the molecular level can affect electronic processes within an organic semiconductor thin film, but its ability to image the active layers of OLED devices directly is limited. In STM experiments in which electrons need to tunnel through the sample to the tip, only very thin organic semiconductor films composed of—at most—several molecular layers can be examined because of the inherent resistivity of the material. However, active layers in OTFTs are frequently at least 50 nm and in OLEDs and OPVs 100–200 nm thick. Although at first glance the thickness of organic semiconductors may seem like an unimportant parameter, extensive reports on pentacene have shown that the organic semiconductor adopts different polymorphs depending on the film thickness (43–46). Morphological information about molecular layers obtained via STM may thus not be representative of active layers composed of the same molecules. To make matters worse, the organic semiconductor of interest must be deposited on a conductive surface to prevent charge accumulation during STM measurements (47–50). This process is incongruent with actual active layers in OTFTs, which are deposited on insulating dielectrics.

Visualization of the molecular ordering in actual active layers of organic electronic devices has proven to be a challenging task, but at the same time is critical to understanding structure-function relationships in organic electronics. For example, low-dose high-resolution electron microscopy (LD-HREM) experiments reveal direct evidence for the presence of many defects within a single pentacene nanocrystal, including lattice curvature and dislocations (**Figure 3**) (51). These defects, if present in the active layers of pentacene OTFTs, could result in a decrease in charge transport through the active layers. Like STM imaging, however, the limitations of LD-HREM and transmission electron microscopy (TEM) more generally have thus far prevented the direct imaging of organic semiconductor active layers at the molecular level. Because TEM collects information from the entire depth of the sample as a 2D projection, the ability to visualize molecular ordering in 50–100 nm films may be lost if the ordering does not extend throughout the depth of the films. TEM experiments also require that the samples be prepared on or transferred to grids to prevent interference of the underlying substrates with the electron beam, processes during which the morphology of the organic semiconductor thin films may be altered. Finally, these imaging techniques only provide local information on the nanometer length scale, whereas the active areas of electronic devices often span millimeters. It is therefore difficult to ascertain if local structural details obtained from TEM and STM span the entire length of the active layers. Not surprisingly, drawing conclusive structure-function relationships from such studies remains difficult.

GRAIN SIZE AND ORIENTATION

In the solid state, extensively conjugated organic semiconductors favor the formation of single crystals that span the active layers. Organic semiconductor thin films, however, are most often polycrystalline, as simultaneous crystallization occurs starting from multiple nucleation sites on substrate surfaces (52). As such, we must consider not only local defects within a single crystalline grain but also how the polygrain nature of organic semiconductor thin films influences charge transport.

In this section, we highlight experiments that demonstrate how grain size and orientation in active layers impact device performance. We also demonstrate the importance of studying the extent of crystallinity and the orientation of the individual constituents within the context of two-component systems. Specifically, in organic semiconductor thin films composed of blends, crystallization and increased grain size of one organic semiconductor are often accompanied by increased phase separation with the other organic semiconductor (41, 53, 54). Such structural

development within the active layers of organic electronic devices has a drastic impact on the details of charge transport. In attempts to quantify such relationships, we point to the novel techniques that have been developed to study grain size and orientation in the active layers of organic electronics.

Impact of Grain Size and Orientation in Single-Component Active Layers on Device Performance

It is generally accepted that intergrain boundaries pose barriers to charge transport; indeed, surface potential measurements on grain boundaries in the active layers of OTFTs composed of polycrystalline copper phthalocyanine (CuPc) (55), sexithiophene (6T) (56), and pentacene (57) all support this claim. Efficient charge transport across active layers thus mandates low grain boundary density or large grains between electrodes. Accordingly, device mobilities generally demonstrate strong, positive correlations with grain size in the active layers of OTFTs (58–60).

To this end, we have demonstrated unprecedented control over grain sizes in TES ADT thin films spanning more than three orders of magnitude, from ~30 μm to ~2700 μm (60). By deliberately introducing seeds to induce crystallization of TES ADT in the form of fluorinated 5,11-bis(triethylsilylethynyl) anthradithiophene (diF-TES ADT) prior to spin coating, we can control the number of nucleation events (and therefore the grain density of TES ADT) that occur in the active layers. When the average grain size in the active layers is 29 μm, OTFTs composed of these films exhibit an average device mobility of 0.005 $cm^2\ V^{-1}\ s^{-1}$, compared with 0.36 $cm^2\ V^{-1}\ s^{-1}$ for OTFTs composed of active layers with an average grain size of 2700 μm. The dependence of device mobility on grain size in the active layers is accurately modeled by the composite mobilities of the grain and grain boundary, each scaled by their respective sizes (61, 62). That this model describes the data well suggests that the mobility through grain boundaries is several orders of magnitude lower than that through grains, which is consistent with prior surface potential measurements that have identified grain boundaries as trap sites for charge carriers.

Although the ability to grow large grains should improve charge transport, the preferential orientation of a grain with respect to neighboring grains plays an equally important role in determining device performance. Given that charge transport is most efficient in the direction of π-π stacking and reduced along other crystallographic directions (63–65), the efficiency with which charges are transported across active layers that span millimeters thus depends on the orientation details of the grains. In a study carried out on OTFTs composed of poly(3-hexyl)thiophene (P3HT), the device mobility increases by two orders of magnitude when P3HT is oriented with its (010) plane, corresponding to the π-stack direction, along the direction of charge transport, compared with when its (010) plane is perpendicular to the direction of current flow (66). Although charge transport is generally more efficient along the π-stack direction, this rule assumes a conduction pathway from one electrode to the other for current collection. Poor connectivity can further limit intergrain charge transport, eventually leading to a decrease in the device mobility of OTFTs (67). Intergrain connectivity is therefore also an important aspect of structure characterization in these materials.

Provided that the grains in the organic semiconductor thin film are sufficiently large, the average grain size of organic semiconductor thin films can be routinely quantified by optical microscopy (23, 60, 68, 69), scanning electron microscopy (SEM) (59, 70), grazing incidence X-ray diffraction (GIXD) (66, 71), and atomic force microscopy (AFM) (58, 72). To quantify grain size and orientation simultaneously, however, hybrid techniques are required. Puntambekar and coworkers, for example, developed transverse shear microscopy (TSM) (57, 73) to examine the crystal orientation of ultrathin films (1–2 nm) of pentacene.

An adaptation of AFM, TSM takes advantage of the anisotropic elasticity of pentacene crystals along different crystallographic directions. The magnitude of the transverse shear force associated with dragging an AFM tip along different crystallographic directions of a single pentacene crystal is first identified. This information is then used to correlate the orientation of polycrystalline thin films by simultaneously recording the shear force associated with the tip while scanning across the pentacene films. In a conventional AFM image collected on the same film, contrast only exists between the crystals that are growing on the overlayer and grains underneath cannot be easily distinguished (**Figure 4*a***). The image taken with TSM, however, shows striking contrast between the underlying individual pentacene grains owing to elastic anisotropy (**Figure 4*b***).

The ability to visualize individual grains and simultaneously to map their orientation in organic semiconductor thin films is crucial for understanding charge transport in these materials. Combining Kelvin probe force microscopy (KFM) with TSM, Puntambekar and coworkers were able to study the surface potential of pentacene thin films while simultaneously obtaining images of individual grains (57). KFM is an adaptation of AFM in which a conductive tip is used to measure the electrostatic forces on the sample surface. Surface potential maps of these pentacene thin films show large potential wells, approximately −5 to −10 mV, at the grain boundaries. This observation unambiguously confirms the prior general belief that grain boundaries can act as trap sites for charge carriers. These experiments also correspond well to studies that demonstrate that OTFT device mobility decreases with increasing density of grain boundaries in the active layers (58–60).

An exciting area of research emerging in organic electronics is studies that probe the morphology and electronic properties of active layers during device operation. For example, scanning probe techniques have been used to study the active layers of OTFTs during operation (74–77). Our group has demonstrated the use of scanning surface potential microscopy (SSPM) to compare the surface potential drop across the active layers of pentacene OTFTs using gold and a conducting polymer as source and drain electrodes during device operation (75). Surface potential measurements show a higher barrier to charge injection and extraction at gold/pentacene interfaces compared with conducting polymer/pentacene interfaces. Characterization via secondary electron microscopy (SEM) and near-edge X-ray absorption fine structure spectroscopy (NEXAFS) reveals structural disorder across multiple length scales ranging from changes in molecular orientation to discontinuity of pentacene grains across the charge injection and extraction interfaces in devices with gold electrodes. Such defects are not observed in the active layers of devices with conducting polymer electrodes.

Using scanning Kelvin probe microscopy (SKPM), a technique similar to SSPM, Teague and coworkers also observe large potential barriers at grain boundaries in operating OTFTs composed of diF-TES ADT (78). In the absence of any grain boundaries, the researchers find large potential barriers at the electrode/diF-TES ADT interface that are similar to those we observe in pentacene OTFTs. For OTFTs that contain multiple grains in the active layers, additional potential barriers are observed at the intergrain boundaries within the channels of the devices. These images, taken during OTFT device operation, again confirm that grain boundaries pose a significant barrier to charge transport in the active layers of OTFTs. The combination of device testing and structural characterization is powerful as it has, in this case, uniquely pinpointed the origin of reduced current levels in macroscopic device measurements.

Impact of Grain Size and Orientation in Two-Component Active Layers on Device Performance

In two-component systems, the grain size and orientation of each phase must be considered in addition to the degree of phase separation between the two components. For example, through

optical microscopy and GIXD experiments, the effects of P3HT crystallinity on the phase-separation characteristics of P3HT/methanofullerene 6,6-phenyl C_{61}-butyric acid methyl ester (PCBM) thin films were examined (54). Given their relative energy levels, P3HT serves as the electron donor and PCBM as the electron acceptor when this constituent pair is incorporated in OPVs. Using the extent of regioregularity of P3HT as a means of controlling crystallinity (66, 79), researchers have been able to correlate an increase in the crystallinity of P3HT with the simultaneous growth of PCBM crystal size and, accordingly, an increase in the phase separation between P3HT and PCBM (54). Counterintuitively, P3HT crystals are much less oriented in films composed of highly crystalline P3HT compared with films composed of less crystalline P3HT. As illustrated in **Figure 5*a***, the researchers attribute this observation to large PCBM crystals forcing P3HT stacks out of their preferential orientation, whereas smaller PCBM crystals cannot significantly affect the existing orientation of P3HT crystals (**Figure 5*b***). OPVs composed of highly crystalline P3HT in their active layers exhibit a decrease in device efficiency upon thermal annealing, likely a result of a corresponding increase in the extent of phase separation between P3HT and PCBM. This example highlights the importance of studying crystallinity and grain orientation in active layers within the context of larger-scale phase separation to establish accurate structure-function relationships. The influence of phase separation in active layers on device characteristics will be discussed in detail in the following section.

PHASE SEPARATION

Phase separation in thin films composed of organic semiconductor blends can occur in both the lateral and vertical directions with respect to the substrate. Lateral phase separation arises from the chemical incompatibility of the two components. Rapid solvent evaporation during film formation, however, can limit the extent of phase separation. Subsequent annealing of the thin films above the glass transition temperatures of the constituents drives the morphology of the films toward a more phase-separated state.

Given the typical thickness of active layers, the substrate surface energy can also influence the distribution of the individual species along the film depth. Depending on the surface energy of the organic semiconductors in comparison with that of the underlying substrate, the organic semiconductors may preferentially segregate to the air/film interface or the film/substrate interface. Synonymous with lateral composition fluctuations in thin films, this phenomenon has been loosely termed "vertical phase separation" in the organic electronics community. As in the case of lateral phase separation, the extent of vertical phase separation can be kinetically limited by the rate of solvent evaporation from the film and may depend on other factors, such as solvent interactions with the organic semiconductors. Similar to lateral phase separation, precise control over this phenomenon thus remains to be achieved.

In the following section, we review the impact of both lateral and vertical phase separation in active layers on OPV device performance. We also point to recent studies that simultaneously examine vertical and lateral phase separation in organic semiconductor thin films.

Impact of Lateral Phase Separation in Active Layers on Device Performance

In active layers composed of a blend of two organic semiconductors, phase separation between the two components is a critical morphological parameter in determining overall current generation. **Figure 6** shows the electronic processes that occur within the active layers of bulk-heterojunction OPVs. First, light is absorbed within one or both phases in the active layer, resulting in the generation of excitons, or electron-hole pairs. The excitons then need to diffuse to the interface between

the two organic semiconductors. At the interface, the excitons dissociate into electrons and holes. Owing to the built-in electrochemical potential difference within the OPV, electrons are transferred to the electron acceptor phase, whereas holes are transferred to the electron donor phase. Only when electrons and holes travel to and are collected at the cathode and anode, respectively, does the OPV generate current.

From **Figure 6**, it is apparent that the active layers of OPVs should exhibit high interfacial area between the electron donor and electron acceptor for efficient exciton dissociation as well as continuous pathways from the electron donor and acceptor to the anode and cathode, respectively, for effective charge transport to the electrodes. Given the lifetime of an exciton, its diffusion length is on the order of 10 nm in conjugated polymers (80–83). It is widely believed that the characteristic length scale of phase-separated domains in the active layers of OPVs should be comparable with the exciton diffusion length to maximize its dissociation into free carriers.

Because block copolymers tend to microphase separate on a molecular length scale (on the order of tens of nanometers) to form periodic microdomains whose shape and size are tunable through synthetic parameters and which can subsequently be aligned with external fields, they have been proposed for use as active layers in OPVs, with one block acting as the electron acceptor and the other as the electron donor (84).

Early work in this field conducted by the Hadziioannou group demonstrated the potential of using block copolymers as the active layers in OPVs with a poly(*p*-phenylene vinylene) (PPV) block as the electron donor and a C_{60}-functionalized polystyrene segment as the electron acceptor. Compared to devices composed of blends of the constituent homopolymers as the active layers, devices incorporating the block copolymer as the active layer exhibited enhanced, albeit low, photovoltaic response (85, 86). More recently, Lindner and coworkers synthesized a block copolymer consisting of poly(vinyltriphenylamine) (PvTPA) and polyacrylate with perylene bisimide side groups (PPerAcr) as the electron donating and accepting blocks, respectively. Compared with OPVs composed of a blend of PvTPA and PPerAcr as the active layer, OPVs composed of the block copolymer $PvTPA_{21}$-*block*-$PPerAcr_{71}$ show an order of magnitude higher device performance—0.07% compared with 0.007% (87). The increase in device efficiency for OPVs in which a block copolymer is the active layer is attributed to differences in morphology in the active layers: Whereas blends of PvTPA and PPerAcr in thin films phase separate into micron-size domains, $PvTPA_{21}$-*block*-$PPerAcr_{71}$ thin films exhibit domains on the order of tens of nanometers, comparable with the diffusion length of excitons. Still, problems in ordering and aligning the microdomains prevent OPVs composed of these materials from approaching the efficiency of the best OPVs composed of blended organic semiconductors. To date, the highest reported efficiencies of OPVs composed of block copolymers remain well under 1%, compared with 5–6% for the best bulk heterojunction OPVs prepared with blends of a polymer donor and a fullerene derivative as the electron acceptor (88, 89).

In OPVs that incorporate blends of organic semiconductors as the active layers, the phase-separated domains can range from nanometers to microns in length depending on the details of the processing conditions. Controlling the extent of phase separation in these systems has proven challenging, however. Researchers have sought to manipulate phase separation in thin films of organic semiconductor blends by altering the composition of the film by varying the ratios of the two components (90–92); by incorporating additives (93–95); by imposing postprocessing treatments, such as thermal annealing (96–99) and solvent vapor annealing (100); or by controlling the rate of solvent evaporation from the as-cast films (101). One group has demonstrated the ability to tune the phase-separation characteristics of the active layers on a gross level, first forming nanoparticles composed of both the electron donor and acceptor and subsequently depositing a mixture of these particles in thin films (102, 103). Not unexpectedly, such processing techniques and parameters

have also been shown to change the crystallinity in one or both components in organic semiconductor thin films, so the simultaneous study of crystallinity and phase separation in a system is often necessary to correlate the morphology of the active layers to device performance (54, 98, 100).

Previously we highlighted GIXD experiments on thin films composed of blends of P3HT/PCBM that indicate that the degree of phase separation between P3HT (96% regioregular) and PCBM can influence OPV device performance (54). The researchers found that continued thermal annealing of the active layers leads to coarsening of the PCBM domains. This coarsening effectively reduces the interface between P3HT and PCBM at which excitons can dissociate. As a consequence, device efficiencies suffer with extended annealing of the active layers. However, the as-cast active layers exhibit very fine structures with high interdomain interfacing because the processing conditions kinetically hinder phase separation. These devices also exhibit lower efficiencies compared with devices that were moderately annealed because the high interfacial area in this case promotes charge recombination. There thus appears to be an optimal length scale of phase separation at which exciton dissociation is maximized and free carrier recombination is minimized. Given the difficulties associated with controlling phase separation and the technical challenges associated with measuring the interfacial area, this optimal degree of phase separation has yet to be verified. Experiments to date, however, suggest that this optimal length scale could be much larger, on the order of tens to hundreds of nanometers (93, 98, 100), than the 10 nm that is generally thought to be the exciton diffusion length.

Simultaneous grazing-incidence small-angle X-ray scattering (GISAXS) and wide-angle X-ray diffraction (GIWAXD) on as-cast and thermally annealed P3HT/PCBM thin films have also been used to characterize the active layers of P3HT/PCBM OPVs (98). GISAXS can provide information on the extent of phase separation (on the order of tens of nanometers), whereas GIWAXD provides crystallographic information on the individual species at the molecular level. Specifically, GISAXS spectra acquired on films of P3HT/PCBM show an increase in X-ray intensity upon annealing that corresponds to an increase in the PCBM domain size. From this observation, the authors infer an increase in the extent of phase separation between P3HT and PCBM. Simultaneously collected GIWAXD spectra show increased intensity of the Bragg reflections of P3HT, which corresponds to increased crystallinity in the P3HT upon thermal annealing. When the active layer is annealed at 100°C, OPV device efficiency is 1.6% compared with 0.5% for OPVs composed of an as-cast active layer. This improvement in efficiency is associated primarily with an increase in P3HT crystallinity, as indicated by GIWAXD spectra. Subsequent annealing at higher temperatures yields larger PCBM domains but does not further enhance P3HT crystallinity. However, the device efficiencies of OPVs composed of these active layers continue to increase with increasing annealing temperatures of the active layers, indicating that enhanced phase separation between P3HT and PCBM in the active layers can improve OPV performance. These results are initially surprising because the average size of PCBM clusters in the active layers of the highest efficiency devices is approximately 50 nm, much larger than the putative diffusion length of excitons. The researchers hypothesize that the larger PCBM domains improve the connectivity of the electron donor and acceptor phases to the anode and cathode, respectively, thereby improving charge collection.

Consistent with the example above, we found that the device efficiency of OPVs composed of P3HT/PCBM thin films increases when the PCBM domain size is on the order of tens to hundreds of nanometers, significantly larger than the proposed length scale for efficient diffusion (93). Through the incorporation of hydrophobic additives to P3HT/PCBM solutions prior to film deposition, we are able to qualitatively control the degree of phase separation between P3HT and PCBM by altering the thermodynamic interactions between the two phases. **Figure 7**, which displays AFM images of P3HT/PCBM thin films containing (*a*) no additives and

(*b*) fractional amounts of a hydrophobic iridium complex (5 wt%), clearly shows that the incorporation of the hydrophobic additive increases the extent of phase separation in the active layers. The clusters, which are on the order of several hundred nanometers, correspond to PCBM; this assignment is confirmed by energy dispersive X-ray spectroscopy (EDX). Even though the domain size of the PCBM clusters is at least an order of magnitude larger than the exciton diffusion length, we observe a considerable increase in current flow from devices composed of the active layers shown in **Figure 7*b*** compared with devices composed of the active layers shown in **Figure 7*a***.

In another study, the incorporation of alkanethiols into a cosolution of poly[2,6-(4,4-bis-(2-ethylhexyl)-4*H*-cyclopenta[2,1-b;3,4-b′]-dithiophene)-*alt*-4,7-(2,1,3-benzothiadiazole)] (PCPDTBT) and [6,6]-phenyl C_{71}-butyric acid methyl ester (C_{71}-PCBM) prior to deposition (104, 105) was investigated. By incorporating alkanethiols into PCPDTBT/C_{71}-PCBM in chlorobenzene prior to spin coating, the researchers are able to tune the phase-separation characteristics between the two polymers. Because alkanethiols are selective solvents for C_{71}-PCBM and also have higher boiling points compared with chlorobenzene, evaporation of chlorobenzene during structure development leads to the selective aggregation and precipitation of PCPDTBT (105), effectively increasing the extent of phase separation between PCPDTBT and C_{71}-PCBM. Surprisingly, GIWAXD experiments performed on PCPDTBT/C_{71}-PCBM thin films show no change in the crystallinity of PCPDTBT and C_{71}-PCBM with the incorporation of alkanethiols. Furthermore, Fourier-transfer infrared (FTIR) and Raman spectroscopy experiments indicate the absence of alkanethiols after film formation. Together, these observations indicate that the only difference in the morphology of active layers that are spun cast from neat chlorobenzene and those from solutions containing alkanethiols is the degree of phase separation between PCPDTBT and C_{71}-PCBM. Accordingly, the improvement in OPV efficiency can be correlated unambiguously to improved phase separation between the two components in the active layer.

These examples confirm the general belief that increased phase separation between the electron donor and acceptor increases the likelihood of holes and electrons reaching the anode and cathode, respectively, before recombining, thereby improving the current density of the resulting OPVs. Recently, researchers have applied scanning probe techniques, such as conductive and photoconductive AFM (21, 106–108), as well as near-field scanning optical microscopy (NSOM) (99, 109) to collect local morphological information and directly measure photocurrent generation in phase-separated systems simultaneously. Bull and coworkers, for example, used light beam induced current microscopy (LBIC) to study the photocurrent distribution in thin films of poly(5,7-bis(3-dodecylthiophen-2-yl)thieno[3,4-b]pyrazine-*alt*-9,9-dioctyl-2,7-fluorene) (BTTP-F) and PCBM (100). The researchers found that exposure of BTTP-F/PCBM thin films to chlorobenzene vapors for 30 min induces the growth of micron-sized PCBM crystallites. LBIC measurements reveal three distinct regions of photocurrent in annealed films (**Figure 8*a***) compared with uniform photocurrent in unannealed films (**Figure 8*b***). In a representative annealed film, no photocurrent is generated inside the PCBM cluster, labeled region A in **Figure 8*a***. Surrounding the PCBM cluster is a region of high photocurrent, labeled B. Further away from the PCBM cluster, the photocurrent drops, as seen in region C. Despite the nonuniformity in the photocurrent of the annealed film, the overall device efficiency of OPVs composed of such films is 1.25%, compared with 0.75% for OPVs composed of unannealed films. This increase in OPV device efficiency is attributed to the increased exciton dissociation and thus higher free carrier generation in the region labeled B in **Figure 8*a***. Although improved crystallinity in the PCBM domain may allow for improved local transport of electrons, it is the dissociation of charges at the interface that most impacts OPV device performance. Such results emphasize the importance of studying the active layer morphology at different length scales as they relate to the different electronic processes in OPV operation.

Impact of Vertical Phase Separation in Active Layers on Device Performance

Vertical phase separation of two organic semiconductors in the active layers of organic electronic devices can also play an important role in determining device performance. In the case of bulk-heterojunction OPVs, for example, electrons that are generated in the active layers must travel through the electron acceptor phase to the cathode, and holes must travel through the electron donor phase to the anode to generate current. Enhancement of the electron donor at the anode will provide greater selectivity for holes, and likewise enhancement of the electron acceptor at the cathode will provide greater selectivity for electrons, effectively increasing the device short circuit current, J_{sc}. Similar concepts apply in OLED devices; preferential segregation of the p-type organic semiconductor to the anode and the n-type organic semiconductor to the cathode can enhance hole and electron injection, respectively, into the active layers. Although the role of vertical phase separation in the active layers of OLEDs has not been extensively studied (110, 111), researchers in this field have been known to incorporate hole transport layers beside the anode and electron transport layers beside the cathode to facilitate charge injection into the light-emitting layers (3).

Vertical phase separation in organic semiconductor thin films has been studied, especially in the context of OPVs, by a variety of methods, including SEM and TEM (91, 112–114), X-ray photoelectron spectroscopy (XPS) (115), NEXAFS (116), Rutherford backscattering spectroscopy (RBS) (90), nuclear reaction analysis (NRA) (110, 117), and secondary ion mass spectrometry (SIMS) (118). Through the use of variable-angle spectroscopic ellipsometry (VASE), Campoy-Quiles and coworkers examined the vertical phase separation characteristics of thin films composed of P3HT/PCBM blends deposited on a hydrophilic substrate (119). In as-cast films, PCBM preferentially segregates to the film/substrate interface, whereas P3HT segregates to the film/air interface. Post-processing treatments, such as thermal annealing, controlled solvent evaporation from the film after deposition, and solvent vapor annealing, increase segregation; further enhancement of PCBM at the film/substrate interface is observed. Microscopy experiments carried out on these films reveal that this change in the vertical composition profile of the films occurs simultaneously with an increase in P3HT crystallinity and enhanced lateral phase separation between PCBM and P3HT, illustrating yet again how the structures at different length scales are intertwined. Teasing out the morphology in P3HT/PCBM active layers that is responsible for enhancements in OPV device efficiencies is thus complex and challenging.

Recently, our group used NEXAFS to quantify the vertical phase separation in P3HT/PCBM films deposited on a hydrophilic substrate. By also examining films of P3HT/PCBM that had been delaminated from the underlying substrate, we were able to collect photoelectron yield (PEY) data from both the exposed and the previously buried surfaces of the films. Given that NEXAFS provides a fingerprint spectrum that is unique to the individual constituents, we are able to quantify directly the composition at the exposed and buried interfaces. Quantification of the NEXAFS spectra collected at the carbon edge indicates that PCBM is indeed enriched at the film/substrate interface, whereas P3HT is enriched at the air/substrate interface. These results are consistent with those reported by Campoy-Quiles and coworkers, and are congruent with the observed difference in surface energy between P3HT, which is hydrophobic, and the hydrophilic underlying substrate.

Simultaneous Examination of Lateral and Vertical Phase Separation in the Active Layers

In most studies of phase separation in the active layers of OPVs, vertical phase separation and lateral phase separation are observed independent of one another. Research has shown, however, that the

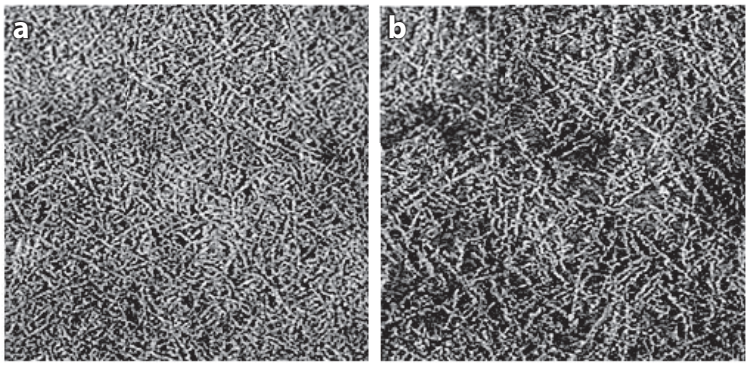

Figure 9

Two-dimensional slices of a reconstructed 3D electron tomography image of P3HT/PCBM thin films (*a*) near the film/substrate interface and (*b*) near the film/air interface. Reprinted with permission from Reference 120. Copyright © 2009 American Chemical Society.

extent of lateral phase separation in an organic semiconductor thin film can vary along the depth of the film as well. For example, in a study of thin films composed of blends of poly[2-methoxy-5-(3′,7′-dimethyloctyloxy)-1,4-phenylene vinylene] (MDMO-PPV) and PCBM, researchers used a high-energy ion beam to sputter the films to depths of 25 nm and 90 nm (90). The morphology of the sputtered films was then characterized by AFM. At the deeper point in the films, larger domains are clearly observed, although dynamic SIMS measurements that were carried out on these films show no change in the vertical composition profile of MDMO-PPV and PCBM. That the overall composition is constant along the depth of the film at the resolution achievable by SIMS suggests that the density and size of the phase-separated domains are changing with film depth.

Recently, van Bavel and coworkers have demonstrated the use of electron tomography to reconstruct the perceived morphology of thin films composed of blends of P3HT/PCBM in three dimensions from 2D images acquired at many film depths (120). This development has allowed the examination of lateral phase separation as a function of the depth of the film. Additionally, because the electron density between crystalline P3HT and PCBM is sufficiently high to observe individual P3HT crystalline fibers, the crystallinity of P3HT can be estimated as a function of film depth. **Figure 9** shows 2D slices taken from the 3D reconstructed electron tomography image of P3HT/PCBM thin films near the film/substrate interface (*a*) and the film/air interface (*b*). By taking a series of 2D slices along the depth of the electron tomography image, the researchers were able to build a composition profile along the depth of the film. In thermally annealed P3HT/PCBM thin films, the composition profile reveals a higher density of P3HT fibers near the film/substrate interface compared with the film/air interface. The researchers also approximate that 60% of the P3HT is crystalline, based on the volume fraction of P3HT fibers and respective densities of P3HT and PCBM.

Based on these electron tomography studies, the researchers hypothesize that P3HT aggregates sink to the film/substrate interface during solution deposition and subsequently nucleate the growth of P3HT crystals, resulting in an increase in P3HT crystals at the film/substrate interface (120). Given the size of these aggregates (on the order of 100 nm), however, it is questionable how large a role gravity plays during structure development. Somewhat surprisingly, these results contradict previous work, including our own, on vertical phase separation in P3HT/PCBM thin films, which indicates an enrichment of PCBM at the film/substrate interface and an enrichment

of P3HT at the air/film interface when the polymers are deposited on hydrophilic substrates (119, 121).

Despite reporting differences in the vertical phase separation between P3HT and PCBM in the active layers of OPVs, high-resolution 3D imaging of the active layers of bulk-heterojunction OPVs can reveal morphological details previously inaccessible via other techniques. The development of electron tomography and related imaging techniques remains challenging, however, because organics generally have similar electron densities, which drastically reduces contrast. Whereas crystalline P3HT fibers are easily distinguishable in the prior example, there is insufficient electron density contrast between amorphous P3HT and PCBM (120). Such techniques also generally lack the resolution needed to image the fibers at the molecular level. Defects and grain boundaries within the fibers themselves can affect charge transport (67), so a more detailed investigation would be needed to elucidate morphology at this length scale.

OUTLOOK

Although characterization tools, such as STM, TSM, and LBIC, have greatly enhanced our understanding of how morphology at individual length scales can influence electronic processes within active layers, we still lack a comprehensive understanding of how these morphological considerations across all length scales link together to determine the overall device performance. Specifically, we lack the capability to study the hierarchical structuring that transverses the subnanometer to millimeter length scales in the active layers of organic electronics as it pertains to overall device characteristics. As demonstrated in this review, important morphological considerations exist over this entire range of length scales. Although many studies have addressed how morphology at a single length scale in active layers can impact individual electronic processes, ample evidence demonstrates that structuring is intertwined over multiple length scales. As we have seen, changes in molecular ordering can impact grain size and orientation, which in turn can affect the degree of phase separation between two components in active layers. Comprehensive studies that employ different characterization tools to study the morphological development of the active layers across multiple length scales in situ would therefore contribute tremendously to the elucidation of structure-function relationships in the field of organic electronics.

Looking forward, the capability to determine device characteristics a priori through, for example, the design of new molecules with prespecified properties or the use of specific processing conditions to control structure development in the active layers will lead to the realization of "electronics anywhere" (17). Research has begun to move in this direction with the development of experiments that relate the thermodynamic properties of materials in active layers directly to device performance. For example, Müller and coworkers employed differential scanning calorimetry to map the phase behavior of P3HT/PCBM blends (122). The researchers found that by blending P3HT and PCBM in active layers at a ratio slightly above the eutectic point (PCBM-rich), optimal OPV device performance could be achieved. Such a composition ratio allows for the formation of PCBM-rich domains within a network of finely mixed P3HT and PCBM. This morphology is hypothesized to aid in balanced charge transport by providing continuous PCBM networks through the active layers. Although this study focuses mainly on P3HT/PCBM systems, the general concept of using the phase behavior of two components to determine optimal mixing ratios in the active layers of OPVs should be generally applicable to other organic semiconductor blends.

Recently, we have shown that we can alter the interaction parameter, χ, between the P3HT-rich and PCBM phases by the incorporation of hydrophobic additives into active layers. By changing the chemical incompatibility between the two phases, we could influence the degree of phase separation in P3HT/PCBM thin films (**Figure 7**). The OPV device performance, in particular the J_{sc}, is

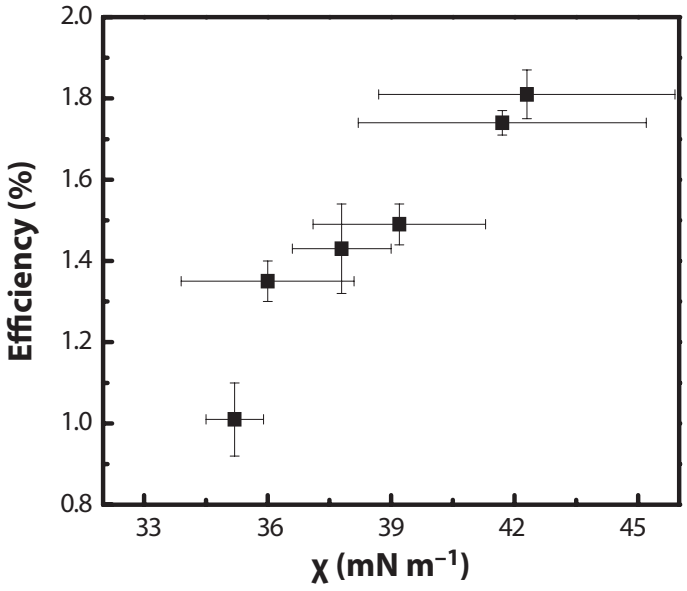

Figure 10

Dependence of OPV device efficiency on the interaction parameter, χ, between the P3HT-rich and PCBM phases in the active layer (93). Copyright © Wiley-VCH Verlag GmbH & Co. KGaA. Reproduced with permission.

strongly correlated to χ, as seen in **Figure 10** (93). These results suggest that the quantification of χ, based in principle on the inherent materials properties of organic semiconductors, can provide some level of predictability of the device performance of OPVs composed of these components.

The ease with which organic semiconductors can be derivatized and functionalized leads to the tunability of their properties. Experiments that correlate the inherent properties of the organics in active layers to device performance should thus generate guidelines, allowing us to progress toward the ability to predict device performance prior to fabrication. Chemical engineers with expertise in material properties and thermodynamics are particularly well-equipped to contribute to this means of elucidating processing-structure-function relationships in organic electronic devices. Ultimately, the ability to develop a set of materials guidelines and procedures to achieve optimal device performance in OTFTs, OPVs, and OLEDs will drive progress in the field of organic electronics.

DISCLOSURE STATEMENT

The authors are not aware of any affiliations, memberships, funding, or financial holdings that might be perceived as affecting the objectivity of this review.

ACKNOWLEDGMENTS

S.S.L. gratefully acknowledges support from a NDSEG Graduate Fellowship through the U.S. Department of Defense. We also thank the Beckman Foundation, the ONR Photovoltaics Program (N000140811175), and the National Science Foundation MRSEC Program through the Princeton Center for Complex Materials (DMR-0819860) for funding.

LITERATURE CITED

1. Sirringhaus H, Tessler N, Friend RH. 1998. Integrated optoelectronic devices based on conjugated polymers. *Science* 280:1741–44
2. Gelinck GH, Huitema HEA, van Veenendaal E, Cantatore E, Schrijnemakers L, et al. 2004. Flexible active-matrix displays and shift registers based on solution-processed organic transistors. *Nat. Mater.* 3:106–10
3. Geffroy B, le Roy P, Prat C. 2006. Organic light-emitting diode (OLED) technology: materials, devices and display technologies. *Polym. Int.* 55:572–82
4. Rotzoll R, Mohapatra S, Olariu V, Wenz R, Grigas M, et al. 2006. Radio frequency rectifiers based on organic thin-film transistors. *Appl. Phys. Lett.* 88:123502–3
5. Steudel S, Myny K, Arkhipov V, Deibel C, De Vusser S, et al. 2005. 50 MHz rectifier based on an organic diode. *Nat. Mater.* 4:597–600
6. Torsi L. 2006. Organic thin-film transistors as analytical and bioanalytical sensors. *Anal. Bioanal. Chem.* 384:309
7. Mabeck J, Malliaras G. 2006. Chemical and biological sensors based on organic thin-film transistors. *Anal. Bioanal. Chem.* 384:343–53
8. Thompson BC, Fréchet JMJ. 2008. Polymer-fullerene composite solar cells. *Angew. Chem. Int. Ed.* 47:58–77
9. Kim JY, Lee K, Coates NE, Moses D, Nguyen T-Q, et al. 2007. Efficient tandem polymer solar cells fabricated by all-solution processing. *Science* 317:222–25
10. Loo Y-L. 2007. Solution-processable organic semiconductors for thin-film transistors: opportunities for chemical engineers. *AIChE J.* 53:1066–74
11. Loo Y-L, McCulloch I. 2008. Progress and challenges in commercialization of organic electronics. *MRS Bull.* 33:653
12. Forrest SR. 2004. The path to ubiquitous and low-cost organic electronic appliances on plastic. *Nature* 428:911–18
13. Rogers JA, Bao Z. 2002. Printed plastic electronics and paperlike displays. *J. Polym. Sci. Part A* 40:3327–34
14. Yan H, Chen Z, Zheng Y, Newman C, Quinn JR, et al. 2009. A high-mobility electron-transporting polymer for printed transistors. *Nature* 457:679–86
15. Sirringhaus H, Kawase T, Friend RH, Shimoda T, Inbasekaran M, et al. 2000. High-resolution inkjet printing of all-polymer transistor circuits. *Science* 290:2123–26
16. Brabec CJ, Durrant JR. 2008. Solution-processed organic solar cells. *MRS Bull.* 33:670
17. Jackson TN. 2002. Organic thin film electronics—electronics anywhere. *Abstr. Pap. Am. Chem. Soc.* 223:069-PHYS
18. Sze SM. 2002. *Semiconductor Devices: Physics and Technology*. New York: Wiley
19. Moulé AJ, Meerholz K. 2009. Morphology control in solution-processed bulk-heterojunction solar cell mixtures. *Adv. Funct. Mater.* 19(10):3028–36
20. Hou J, Chen HY, Zhang S, Chen RI, Yang Y, et al. 2009. Synthesis of low band gap polymer and its application in highly efficient polymer solar cells. *J. Am. Chem. Soc.* 131:15586–87
21. Coffey DC, Reid OG, Rodovsky DB, Bartholomew GP, Ginger DS. 2007. Mapping local photocurrents in polymer/fullerene solar cells with photoconductive atomic force microscopy. *Nano Lett.* 7:738–44
22. Kietzke T, Neher D, Kumke M, Montenegro R, Landfester K, Scherf U. 2004. A nanoparticle approach to control the phase separation in polyfluorene photovoltaic devices. *Macromolecules* 37:4882–90
23. Dickey KC, Anthony JE, Loo Y-L. 2006. Improving organic thin-film transistor performance through solvent-vapor annealing of solution-processable triethylsilylethynyl anthradithiophene. *Adv. Mater.* 18:1721–26
24. Dickey KC, Smith TJ, Stevenson KJ, Subramanian S, Anthony JE, Loo Y-L. 2007. Establishing efficient electrical contact to the weak crystals of triethylsilylethynyl anthradithiophene. *Chem. Mater.* 19:5210–15
25. Dickey KC, Subramanian S, Anthony JE, Han L-H, Chen S, Loo Y-L. 2007. Large-area patterning of a solution-processable organic semiconductor to reduce parasitic leakage and off currents in thin-film transistors. *Appl. Phys. Lett.* 90:244103

26. Era M, Tsutsui T, Saito S. 1995. Polarized electroluminescence from oriented p-sexiphenyl vacuum-deposited film. *Appl. Phys. Lett.* 67:2436–8
27. Chen XL, Lovinger AJ, Bao Z, Sapjeta J. 2001. Morphological and transistor studies of organic molecular semiconductors with anisotropic electrical characteristics. *Chem. Mater.* 13:1341–48
28. Kang SJ, Noh YY, Baeg KJ, Ghim J, Park JH, et al. 2008. Effect of rubbed polyimide layer on the field-effect mobility in pentacene thin-film transistors. *Appl. Phys. Lett.* 92:052107
29. Chou WY, Cheng HL. 2004. An orientation-controlled pentacene film aligned by photoaligned polyimide for organic thin-film transistor applications. *Adv. Funct. Mater.* 14:811–15
30. Jin SH, Seo HU, Nam DH, Shin WS, Choi JH, et al. 2005. Surface-induced alignment of pentacene by photo-alignment technology for organic thin film transistors. *J. Mater. Chem.* 15:5029–36
31. Dyreklev P, Gustafsson G, Inganäs O, Stubb H. 1993. Polymeric field effect transistors using oriented polymers. *Synth. Met.* 57:4093–98
32. Kang SJ, Noh M, Park DS, Kim HJ, Whang CN, Chang CH. 2004. Influence of postannealing on polycrystalline pentacene thin film transistor. *J. Appl. Phys.* 95:2293–96
33. Yang H, Shin TJ, Bao Z, Ryu CY. 2007. Structural transitions of nanocrystalline domains in regioregular poly(3-hexyl thiophene) thin films. *J. Polym. Sci. Part B* 45:1303–12
34. Jo SJ, Kim CS, Lee MJ, Kim JB, Ryu SY, et al. 2008. Inducement of azimuthal molecular orientation of pentacene by imprinted periodic groove patterns for organic thin-film transistors. *Adv. Mater.* 20:1146–53
35. Onoki R, Yoshikawa G, Tsuruma Y, Ikeda S, Saiki K, Ueno K. 2008. Nanotransfer of the polythiophene molecular alignment onto the step-bunched vicinal Si(111) substrate. *Langmuir* 24:11605–10
36. Xu G, Bao Z, Groves JT. 2000. Langmuir-Blodgett films of regioregular poly(3-hexylthiophene) as field-effect transistors. *Langmuir* 16:1834–41
37. Cimrová V, Remmers M, Neher D, Wegner G. 1996. Polarized light emission from LEDs prepared by the Langmuir-Blodgett technique. *Adv. Mater.* 8:146–49
38. Weng SZ, Hu WS, Kuo CH, Tao YT, Fan LJ, Yang YW. 2006. Anisotropic field-effect mobility of pentacene thin-film transistor: effect of rubbed self-assembled monolayer. *Appl. Phys. Lett.* 89:172103
39. Hu WS, Weng SZ, Tao YT, Liu HJ, Lee HY, et al. 2007. Oriented growth of crystalline pentacene films with preferred a-b in-plane alignment on a rubbed crystalline polymethylene surface. *Langmuir* 23:12901–9
40. Stohr J, Samant MG, Cossy-Favre A, Diaz J, Momoi Y, et al. 1998. Microscopic origin of liquid crystal alignment on rubbed polymer surfaces. *Macromolecules* 31:1942–46
41. Gong JR, Wan LJ, Lei SB, Bai CL, Zhang XH, Lee ST. 2005. Direct evidence of molecular aggregation and degradation mechanism of organic light-emitting diodes under joule heating: an STM and photoluminescence study. *J. Phys. Chem. B* 109:1675–82
42. McNeill CR, Greenham NC. 2009. Conjugated-polymer blends for optoelectronics. *Adv. Mater.* 21: 3840–50
43. Dimitrakopoulos CD, Brown AR, Pomp A. 1996. Molecular beam deposited thin films of pentacene for organic field effect transistor applications. *J. Appl. Phys.* 80:2501–8
44. Minakata T, Imai H, Ozaki M, Saco K. 1992. Structural studies on highly ordered and highly conductive thin films of pentacene. *J. Appl. Phys.* 72:5220–25
45. Ruiz R, Mayer AC, Malliaras GG, Nickel B, Scoles G, et al. 2004. Structure of pentacene thin films. *Appl. Phys. Lett.* 85:4926–28
46. Mayer AC, Kazimirov A, Malliaras GG. 2006. Dynamics of bimodal growth in pentacene thin films. *Phys. Rev. Lett.* 97:105503
47. Alvarado SF, Rossi L, Müller P, Rieß W. 2001. Charge-carrier injection into CuPc thin films: a scanning tunneling microscopy study. *Synth. Met.* 122:73–77
48. France CB, Schroeder PG, Forsythe JC, Parkinson BA. 2003. Scanning tunneling microscopy study of the coverage-dependent structures of pentacene on Au(111). *Langmuir* 19:1274–81
49. France CB, Schroeder PG, Parkinson BA. 2002. Direct observation of a widely spaced periodic row structure at the pentacene/Au(111) interface using scanning tunneling microscopy. *Nano Lett.* 2:693–96
50. Braun D, Schirmeisen A, Fuchs H. 2005. Molecular growth and submolecular resolution of a thin multilayer of PTCDA on Ag(110) observed by scanning tunneling microscopy. *Surf. Sci.* 575:3–11

51. Drummy LF, Kübel C, Lee D, White A, Martin DC. 2002. Direct imaging of defect structures in pentacene nanocrystals. *Adv. Mater.* 14:54–57
52. Heringdorf FJM, Reuter MC, Tromp RM. 2001. Growth dynamics of pentacene thin films. *Nature* 412:517–20
53. Motaung DE, Malgas GF, Arendse CJ, Mavundla SE, Oliphant CJ, Knoesen D. 2009. The influence of thermal annealing on the morphology and structure properties of a conjugated polymer in blends with an organic acceptor material. *J. Mater. Sci.* 44:3192–97
54. Woo CH, Thompson BC, Kim BJ, Toney MF, Fréchet JMJ. 2008. The influence of poly(3-hexylthiophene) regioregularity on fullerene-composite solar cell performance. *J. Am. Chem. Soc.* 130:16324–29
55. Huang H, Wang H, Zhang J, Yan D. 2009. Surface potential images of polycrystalline organic semiconductors obtained by Kelvin probe force microscopy. *Appl. Phys. A* 95:125–30
56. Kelley TW, Frisbie CD. 2001. Gate voltage dependent resistance of a single organic semiconductor grain boundary. *J. Phys. Chem. B* 105:4538–40
57. Puntambekar K, Dong J, Haugstad G, Frisbie CD. 2006. Structural and electrostatic complexity at a pentacene/insulator interface. *Adv. Funct. Mater.* 16:879–84
58. Di Carlo A, Piacenza F. 2005. Influence of grain sizes on the mobility of organic thin-film transistors. *Appl. Phys. Lett.* 86:263501
59. Horowitz G, Hajlaoui ME. 2001. Grain size dependent mobility in polycrystalline organic field-effect transistors. *Synth. Met.* 122:185–89
60. Lee SS, Kim CS, Gomez ED, Purushothaman B, Toney MF, et al. 2009. Controlling nucleation and crystallization in solution-processed organic semiconductors for thin-film transistors. *Adv. Mater.* 35:3605–9
61. Farmakis FV, Brini J, Kamarinos G, Angelis CT, Dimitriadis CA, Miyasaka M. 2001. On-current modeling of large-grain polycrystalline silicon thin-film transistors. *IEEE Trans. Electron Devices* 48:701
62. Horowitz G. 2004. Organic thin film transistors: from theory to real devices. *J. Mater. Res.* 19:1946–62
63. Lee JY, Roth S, Park YW. 2006. Anisotropic field effect mobility in single crystal pentacene. *Appl. Phys. Lett.* 88:252106
64. Sundar VC, Zaumseil J, Podzorov V, Menard E, Willett RL, et al. 2004. Elastomeric transistor stamps: reversible probing of charge transport in organic crystals. *Science* 303:1644–46
65. Kim DH, Park YD, Jang Y, Yang H, Kim YH, et al. 2005. Enhancement of field-effect mobility due to surface-mediated molecular ordering in regioregular polythiophene thin film transistors. *Adv. Funct. Mater.* 15:77–82
66. Sirringhaus H, Brown PJ, Friend RH, Nielsen MM, Bechgaard K, et al. 1999. Two-dimensional charge transport in self-organized, high-mobility conjugated polymers. *Nature* 401:685–88
67. Jimison LH, Toney MF, McCulloch I, Heeney M, Salleo A. 2009. Charge-transport anisotropy due to grain boundaries in directionally crystallized thin films of regioregular poly(3-hexylthiophene). *Adv. Mater.* 21:1568–72
68. Chen J, Martin DC, Anthony JE. 2007. Morphology and molecular orientation of thin-film bis(triisopropylsilylethynyl) pentacene. *J. Mater. Res.* 22:1701–9
69. Kim CS, Lee S, Gomez ED, Anthony JE, Loo Y-L. 2008. Solvent-dependent electrical characteristics and stability of organic thin-film transistors with drop cast bis(triisopropylsilylethynyl) pentacene. *Appl. Phys. Lett.* 93:103302
70. Horowitz G, Hajlaoui ME. 2000. Mobility in polycrystalline oligothiophene field-effect transistors dependent on grain size. *Adv. Mater.* 12:1046–50
71. Nikitenko VR, Heil H, von Seggern H. 2003. Space-charge limited current in regioregular poly-3-hexylthiophene. *J. Appl. Phys.* 94:2480–85
72. Knipp D, Street RA, Volkel A, Ho J. 2003. Pentacene thin film transistors on inorganic dielectrics: morphology, structural properties, and electronic transport. *J. Appl. Phys.* 93:347–55
73. Kalihari V, Tadmor EB, Haugstad G, Frisbie CD. 2008. Grain orientation mapping of polycrystalline organic semiconductor films by transverse shear microscopy. *Adv. Mater.* 20:4033–39
74. Nichols JA, Gundlach DJ, Jackson TN. 2003. Potential imaging of pentacene organic thin-film transistors. *Appl. Phys. Lett.* 83:2366–68

75. Lee KS, Smith TJ, Dickey KC, Yoo JE, Stevenson KJ, Loo Y-L. 2006. High-resolution characterization of pentacene/polyaniline interfaces in thin-film transistors. *Adv. Funct. Mater.* 16:2409–14
76. Puntambekar KP, Pesavento PV, Frisbie CD. 2003. Surface potential profiling and contact resistance measurements on operating pentacene thin-film transistors by Kelvin probe force microscopy. *Appl. Phys. Lett.* 83:5539–41
77. Seshadri K, Frisbie CD. 2001. Potentiometry of an operating organic semiconductor field-effect transistor. *Appl. Phys. Lett.* 78:993–95
78. Teague LC, Hamadani BH, Jurchescu OD, Subramanian S, Anthony JE, et al. 2008. Surface potential imaging of solution processable acene-based thin film transistors. *Adv. Mater.* 20:4513–16
79. Kim Y, Cook S, Tuladhar SM, Choulis SA, Nelson J, et al. 2006. A strong regioregularity effect in self-organizing conjugated polymer films and high-efficiency polythiophene:fullerene solar cells. *Nat. Mater.* 5:197–203
80. Halls JJM, Pichler K, Friend RH, Moratti SC, Holmes AB. 1996. Exciton diffusion and dissociation in a poly(p-phenylenevinylene)/C_{60} heterojunction photovoltaic cell. *Appl. Phys. Lett.* 68:3120
81. Halls JJM, Friend RH. 1997. The photovoltaic effect in a poly(p-phenylenevinylene)/perylene heterojunction. *Synth. Met.* 85:1307–8
82. Haugeneder A, Neges M, Kallinger C, Spirkl W, Lemmer U, et al. 1999. Exciton diffusion and dissociation in conjugated polymer/fullerene blends and heterostructures. *Phys. Rev. B* 59:15346–51
83. Stübinger T, Brütting W. 2001. Exciton diffusion and optical interference in organic donor-acceptor photovoltaic cells. *J. Appl. Phys.* 90:3632
84. Darling SB. 2009. Block copolymers for photovoltaics. *Energy Environ. Sci.* 2:1266–73
85. Stalmach U, de Boer B, Videlot C, van Hutten PF, Hadziioannou G. 2000. Semiconducting diblock copolymers synthesized by means of controlled radical polymerization techniques. *J. Am. Chem. Soc.* 122:5464–72
86. de Boer B, Stalmach U, van Hutten PF, Melzer C, Krasnikov VV, Hadziioannou G. 2001. Supramolecular self-assembly and opto-electronic properties of semiconducting block copolymers. *Polymer* 42:9097–109
87. Lindner SM, Hüttner S, Chiche A, Thelakkat M, Krausch G. 2006. Charge separation at self-assembled nanostructured bulk interface in block copolymers. *Angew. Chem. Int. Ed.* 45:3364–68
88. Zhang Q, Cirpan A, Russell TP, Emrick T. 2009. Donor-acceptor poly(thiophene-block-perylene diimide) copolymers: synthesis and solar cell fabrication. *Macromolecules* 42:1079–82
89. Sommer M, Lindner SM, Thelakkat M. 2007. Microphase-separated donor-acceptor diblock copolymers: influence of HOMO energy levels and morphology on polymer solar cells. *Adv. Funct. Mater.* 17:1493–500
90. van Duren JKJ, Yang X, Loos J, Bulle-Lieuwma CWT, Sieval AB, et al. 2004. Relating the morphology of poly(p-phenylene vinylene)/methanofullerene blends to solar-cell performance. *Adv. Funct. Mater.* 14:425–34
91. Hoppe H, Niggemann M, Winder C, Kraut J, Hiesgen R, et al. 2004. Nanoscale morphology of conjugated polymer/fullerene-based bulk-heterojunction solar cells. *Adv. Funct. Mater.* 14:1005–11
92. Kim JS, Ho PKH, Murphy CE, Friend RH. 2004. Phase separation in polyfluorene-based conjugated polymer blends: lateral and vertical analysis of blend spin-cast thin films. *Macromolecules* 37:2861–71
93. Kim CS, Leonard LT, DiSalle BF, Gomez ED, Lee S, et al. 2009. Altering the thermodynamics of phase separation in inverted bulk-heterojunction organic solar cells. *Adv. Mater.* 21:3110–15
94. Yan Y, Hou J, Zheng X, Gang L, Yang Y. 2008. Effects of solvent mixtures on the nanoscale phase separation in polymer solar cells. *Adv. Funct. Mater.* 18:1783–89
95. Peet J, Soci C, Coffin RC, Nguyen TQ, Mikhailovsky A, et al. 2006. Method for increasing the photoconductive response in conjugated polymer/fullerene composites. *Appl. Phys. Lett.* 89:252105
96. Yang X, Loos J, Veenstra SC, Verhees WJH, Wienk MM, et al. 2005. Nanoscale morphology of high-performance polymer solar cells. *Nano Lett.* 5:579–83
97. Ma W, Yang C, Gong X, Lee K, Heeger AJ. 2005. Thermally stable, efficient polymer solar cells with nanoscale control of the interpenetrating network morphology. *Adv. Funct. Mater.* 15:1617–22
98. Chiu MY, Jeng US, Su CH, Liang KS, Wei KH. 2008. Simultaneous use of small- and wide-angle X-ray techniques to analyze nanometerscale phase separation in polymer heterojunction solar cells. *Adv. Mater.* 20:2573–78

99. Reyes-Reyes M, Kim K, Dewald J, Lopez-Sandoval R, Avadhanula A, et al. 2005. Meso-structure formation for enhanced organic photovoltaic cells. *Org. Lett.* 7:5749–52
100. Bull TA, Pingree LSC, Jenekhe SA, Ginger DS, Luscombe CK. 2009. The role of mesoscopic PCBM crystallites in solvent vapor annealed copolymer solar cells. *ACS Nano* 3:627–36
101. Nilsson S, Bernasik A, Budkowski A, Moons E. 2007. Morphology and phase segregation of spin-casted films of polyfluorene/PCBM blends. *Macromolecules* 40:8291–301
102. Kietzke T, Neher D, Kumke M, Ghazy O, Ziener U, Landfester K. 2007. Phase separation of binary blends in polymer nanoparticles. *Small* 3:1041–48
103. Kietzke T, Neher D, Landfester K, Montenegro R, Guntner R, Scherf U. 2003. Novel approaches to polymer blends based on polymer nanoparticles. *Nat. Mater.* 2:408–12
104. Peet J, Kim JY, Coates NE, Ma WL, Moses D, et al. 2007. Efficiency enhancement in low-bandgap polymer solar cells by processing with alkane dithiols. *Nat. Mater.* 6:497–500
105. Lee JK, Ma WL, Brabec CJ, Yuen J, Moon JS, et al. 2008. Processing additives for improved efficiency from bulk heterojunction solar cells. *J. Am. Chem. Soc.* 130:3619–23
106. Pingree LSC, Reid OG, Ginger DS. 2009. Electrical scanning probe microscopy on active organic electronic devices. *Adv. Mater.* 21:19–28
107. McNeill CR, Dastoor PC. 2006. Photocurrent pattern formation in polymer/methanofullerene blends imaged by near-field scanning photocurrent microscopy. *J. Appl. Phys.* 99:033502
108. McNeill CR, Frohne H, Holdsworth JL, Dastoor PC. 2004. Near-field scanning photocurrent measurements of polyfluorene blend devices: directly correlating morphology with current generation. *Nano Lett.* 4:2503–7
109. Klimov E, Li W, Yang X, Hoffmann GG, Loos J. 2006. Scanning near-field and confocal Raman microscopic investigation of P3HT-PCBM systems for solar cell applications. *Macromolecules* 39:4493–96
110. Higgins AM, Martin SJ, Thompson RL, Chappell J, Voigt M, et al. 2005. Surface segregation and self-stratification in blends of spin-cast polyfluorene derivatives. *J. Phys. Condens. Matter* 17:1319–28
111. Moons E. 2002. Conjugated polymer blends: linking film morphology to performance of light emitting diodes and photodiodes. *J. Phys. Condens. Matter* 14:12235–60
112. Hoppe H, Glatzel T, Niggemann M, Hinsch A, Lux-Steiner MC, Sariciftci NS. 2005. Kelvin probe force microscopy study on conjugated polymer/fullerene bulk heterojunction organic solar cells. *Nano Lett.* 5:269–74
113. Hoppe H, Glatzel T, Niggemann M, Schwinger W, Schaeffler F, et al. 2006. Efficiency limiting morphological factors of MDMO-PPV:PCBM plastic solar cells. *Thin Solid Films* 511–512:587–92
114. Martens T, D'Haen J, Munters T, Beelen Z, Goris L, et al. 2003. Disclosure of the nanostructure of MDMO-PPV:PCBM bulk hetero-junction organic solar cells by a combination of SPM and TEM. *Synth. Met.* 138:243–47
115. Yang X, Loos J. 2007. Toward high-performance polymer solar cells: the importance of morphology control. *Macromolecules* 40:1353–62
116. Germack DS, Chan CK, Hamadani BH, Richter LJ, Fischer DA, et al. 2009. Substrate-dependent interface composition and charge transport in films for organic photovoltaics. *Appl. Phys. Lett.* 94:233303
117. Chappell J, Lidzey DG, Jukes PC, Higgins AM, Thompson RL, et al. 2003. Correlating structure with fluorescence emission in phase-separated conjugated-polymer blends. *Nat. Mater.* 2:616–21
118. Svanström CMB, Rysz J, Bernasik A, Budkowski A, Zhang F, et al. 2009. Device performance of APFO-3/PCBM solar cells with controlled morphology. *Adv. Mater.* 21:4398–403
119. Campoy-Quiles M, Ferenczi T, Agostinelli T, Etchegoin PG, Kim Y, et al. 2008. Morphology evolution via self-organization and lateral and vertical diffusion in polymer:fullerene solar cell blends. *Nat. Mater.* 7:158–64
120. van Bavel SS, Sourty E, de With G, Loos J. 2008. Three-dimensional nanoscale organization of bulk heterojunction polymer solar cells. *Nano Lett.* 9:507–13
121. Xu Z, Chen L-M, Yang G, Huang C-H, Hou J, et al. 2009. Vertical phase separation in poly(3-hexylthiophene):fullerene derivative blends and its advantage for inverted structure solar cells. *Adv. Funct. Mater.* 19:1227–34
122. Müller C, Ferenczi TAM, Campoy-Quiles M, Frost JM, Bradley DDC, et al. 2008. Binary organic photovoltaic blends: a simple rationale for optimum compositions. *Adv. Mater.* 20:3510–15

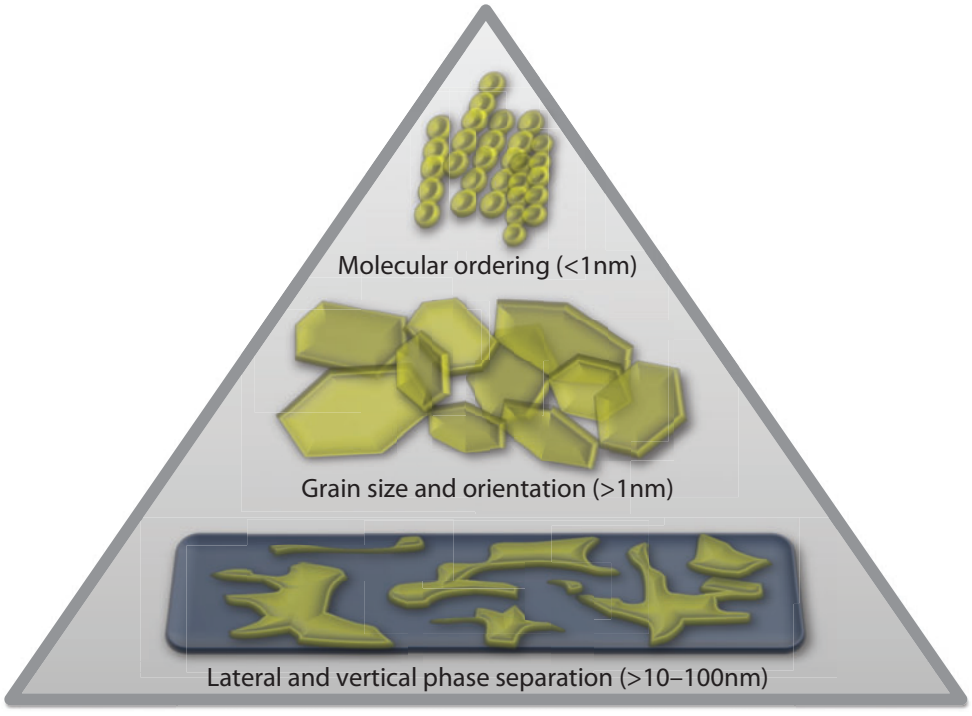

Figure 1

This pyramid displays the three different length scales at which morphological heterogeneities within the active layers of organic electronic devices commonly impact device performance.

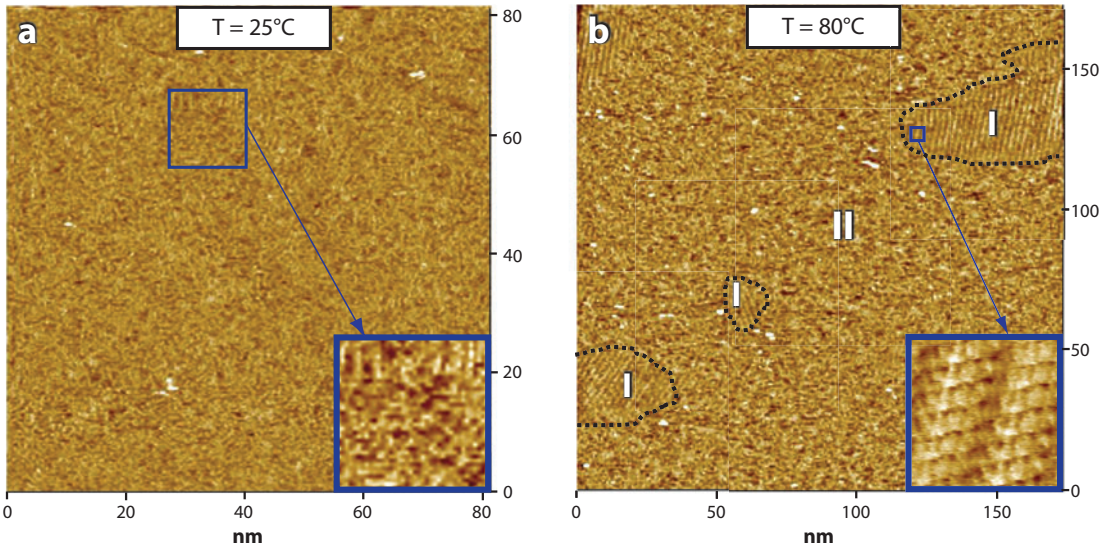

Figure 2

Scanning tunneling microscopy (STM) images of 1,4-bis(benzothiazole-vinyl) benzene/2,2′,2′′-(1,3,5-phenylene)tris-[1-phenyl-1H-benzimidazole] (BT/TPBI) adlayers thermally annealed at (*a*) 25°C and (*b*) 80°C. Labels I and II refer to the crystalline BT phase and amorphous TPBI-rich phase, respectively. Dashed lines added for clarity. Adapted with permission from (41). Copyright © 2005 American Chemical Society.

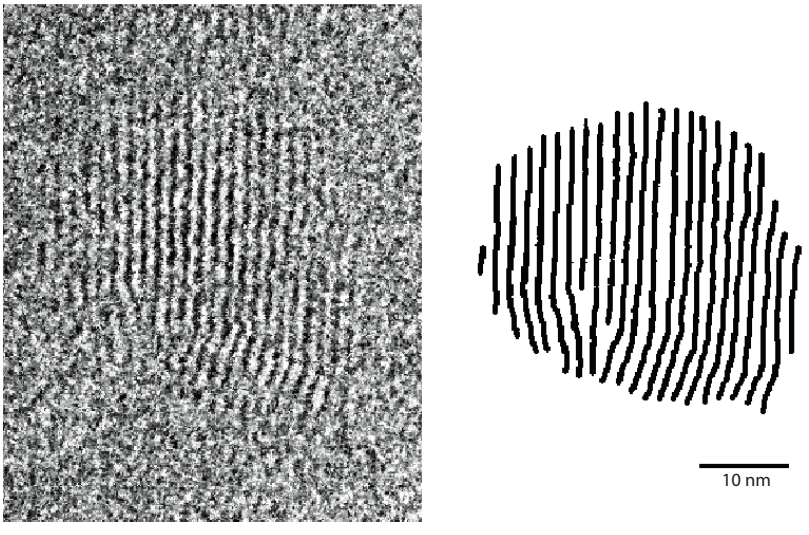

Figure 3

Low-dose high-resolution electron microscopy (LD-HREM) image of a pentacene nanocrystal; lattice fringes are reproduced on the right (51). Copyright © Wiley-VCH Verlag GmbH & Co. KGaA. Reproduced with permission.

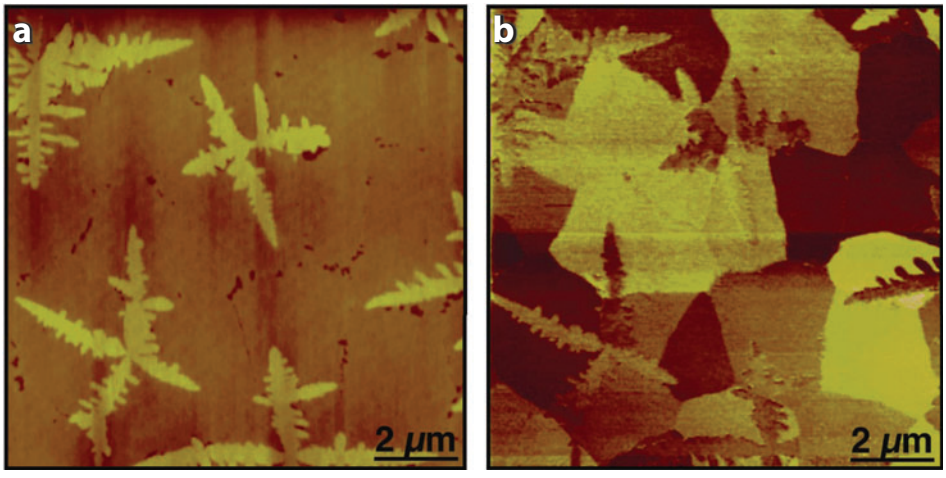

Figure 4

Images of an ultrathin pentacene film acquired by (*a*) atomic force microscopy (AFM) and (*b*) transverse shear microscopy (TSM) (73). Copyright © Wiley-VCH Verlag GmbH & Co. KGaA. Reproduced with permission.

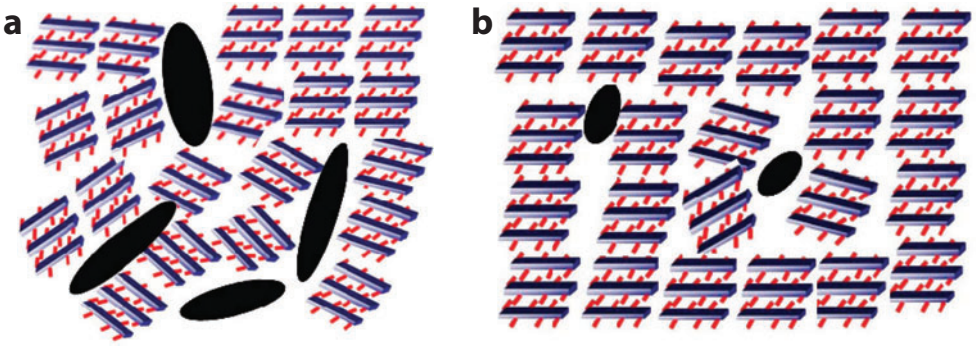

Figure 5

Illustrations of poly(3-hexyl)thiophene (P3HT)/methanofullerene 6,6-phenyl C_{61}-butyric acid methyl ester (PCBM) films composed of (*a*) highly crystalline P3HT and (*b*) less crystalline P3HT. Black circles represent PCBM crystals, and rectangular stacks represent P3HT crystals. Reprinted with permission from (54). Copyright © 2008 American Chemical Society.

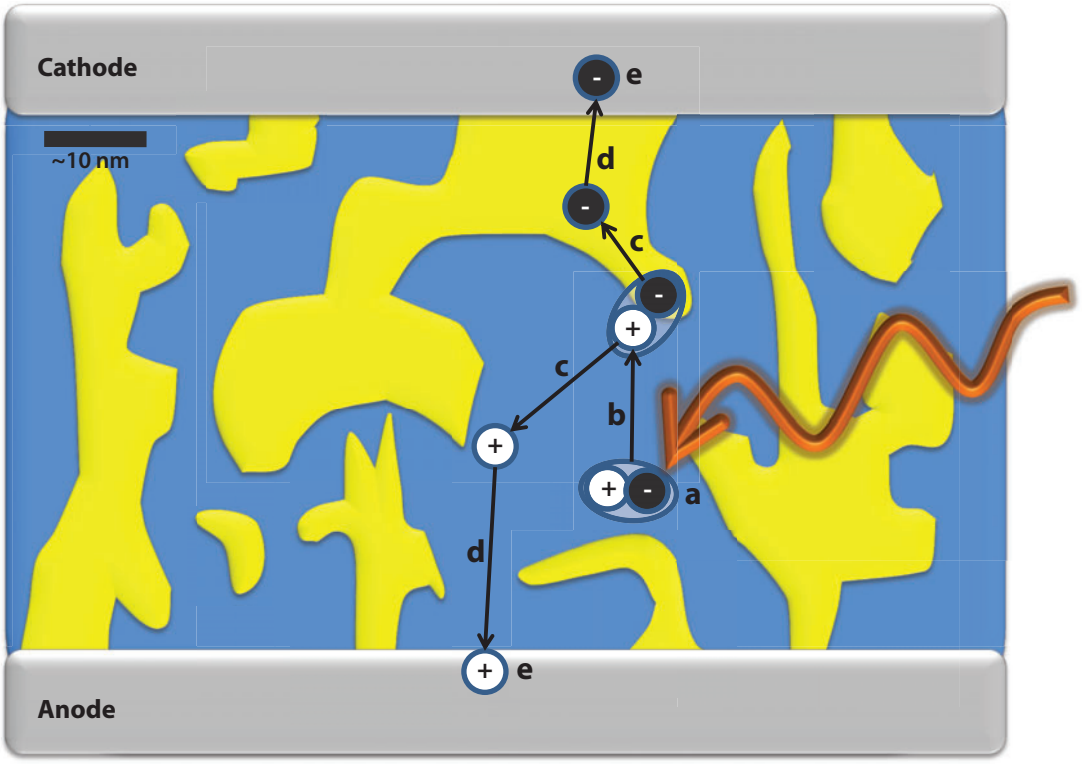

Figure 6

Schematic of a bulk-heterojunction organic photovoltaic (OPV) device. When light is absorbed, excitons are generated (*a*). These excitons need to diffuse to the interfaces of the electron donor and electron acceptor (*b*) for dissociation to occur (*c*). The free carriers that are generated in process c are transported (*d*) and collected at the external electrodes (*e*) to generate photocurrent. Yellow and blue regions indicate the electron acceptor and electron donor phases, respectively.

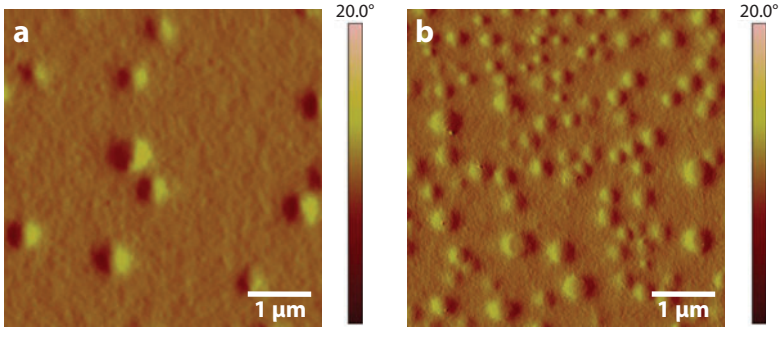

Figure 7

AFM phase images of P3HT/PCBM films with (*a*) no additive and (*b*) the incorporation of fractional amounts of a hydrophobic iridium complex (93). Copyright © Wiley-VCH Verlag GmbH & Co. KGaA. Reproduced with permission.

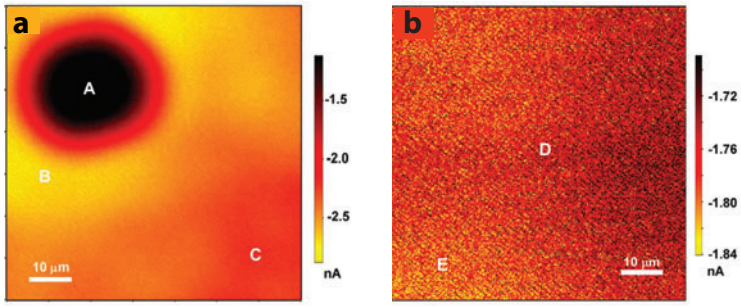

Figure 8

Light beam induced current microscopy (LBIC) images of poly(5,7-bis(3-dodecylthiophen-2-yl)thieno[3,4-b]pyrazine-*alt*-9,9-dioctyl-2,7-fluorene) (BTT-F)/PCBM thin films exposed to chlorobenzene solvent vapors for (*a*) 30 min and (*b*) 0 min. The PCBM cluster, labeled A, is surrounded by a region of high current, labeled B. Farther away from the PCBM cluster exists a region of low photocurrent, labeled C. In unannealed films, photocurrent generation is fairly uniform between regions D and E. Reprinted with permission from (100). Copyright © 2009 American Chemical Society.

Annual Review of Chemical and Biomolecular Engineering

Volume 1, 2010

Contents

Errata

An online log of corrections to *Annual Review of Chemical and Biomolecular Engineering* articles may be found at http://chembioeng.annualreviews.org/errata.shtml